

Quasi-3-day Kelvin wave and the OI(5577Å), OH(6,2) Meinel, and O₂(0,1) emissions

G. S. Lichstein, J. M. Forbes, and M. Angelats i Coll

Department of Aerospace Engineering Sciences, University of Colorado, Boulder, CO, USA

H. Takahashi and D. Gobbi

Instituto Nacional de Pesquisas Espaciais (INPE), São José dos Campos, SP, Brasil

R. A. Buriti

Universidade Federal da Paraíba, Campina Grande, PB, Brasil

Received 24 July 2001; revised 7 January 2002; accepted 7 January 2002; published 26 February 2002.

[1] Ground-based zenith photometric observations at São João do Cariri (7°S, 37°W), Brazil, reveal the existence of ~25–40% quasi-3-day oscillations in OI(5577Å), O₂(0,1), and OH (6,2) emissions and upper mesospheric temperatures (~6K) during June and July, 1998. A previous numerical model study [Forbes, 2000] has reported on the global characteristics of a 3-day Kelvin wave with zonal wavenumber $s = 1$, and consistency with satellite and radar observations. Herein we present the results of a one-dimensional dynamical-chemical simulation that demonstrates that the photometric observations are consistent with a Kelvin wave interpretation. Thus, a connection is made for the first time between convective processes in the tropical troposphere, and upper atmospheric airglow emissions. *INDEX TERMS*: 0341 Atmospheric Composition and Structure: Middle atmosphere—constituent transport and chemistry (3334); 0310 Atmospheric Composition and Structure: Airglow and aurora; 0300 Atmospheric Composition and Structure; 0355 Atmospheric Composition and Structure: Thermosphere—composition and chemistry

1. Introduction

[2] Kelvin waves are the first symmetric eastward propagating “Gravity-Type” oscillations on a sphere [Longuet-Higgins, 1968]; they are confined to equatorial regions, have relatively small meridional velocities, and are primarily excited by tropical convective processes. A recent study by Forbes [2000] utilizes a global-scale numerical model to simulate vertical propagation of a 3-day Kelvin wave with zonal wavenumber $s = 1$ from the lower atmosphere into the thermosphere. This oscillation has an “ultrafast” phase speed compared to other Kelvin waves originating in the tropical troposphere [Salby *et al.*, 1984], and is therefore most likely to penetrate to mesospheric and thermospheric heights. Moreover, its ~56 km vertical wavelength renders it relatively unsusceptible to molecular dissipation until about 110 km. Tropospheric forcing in the model is calibrated to yield agreement with satellite and radar observations of quasi-3-day $s = 1$ oscillations in temperatures and winds in the upper stratosphere and lower thermosphere.

[3] Takahashi *et al.* [2001] present an overview of wave oscillations in zenith airglow photometer measurements made at the equatorial observatory in São João do Cariri (7°S, 37°W), Brazil. Included among these oscillations is a ~3.5-day variation during January, June and July which occurs simultaneously in the

OI(5577Å), O₂(0,1) atmospheric band, and OH (6,2) Meinel band emissions, as well as temperatures inferred from OH band measurements. It is the purpose of the present study to use the wave fields from Forbes [2000] in a dynamical-chemical model to demonstrate consistency of the airglow observations with a Kelvin wave interpretation.

2. The Airglow Model

[4] The one-dimensional finite element model of Angelats *i Coll* and Forbes [1998] has been extended to include HO_x chemistry, and is used here to solve the continuity equations for HO_x (H, OH, HO₂) and O_x (O, O₃) constituent families. The geometry of the model is composed of one column of stacked cells extending from 70 to 200 km. Chemical processes only affect concentrations within a given cell, and transport processes occur between adjacent cells in the vertical direction. The continuity equation solved here for the density N_i of the i th family has the form

$$\frac{\partial N_i}{\partial t} \approx P_i - L_i - \frac{\partial w N_i}{\partial z} \quad (1)$$

where P_i and L_i represent all chemical production and loss processes, z is altitude, and w represents the sum of vertical

Table 1. Chemical Reactions and Rates^a

Reaction	C	A	Source
O+O ₂ + M → O ₃ +M	6.0×10^{-34}	-2.3	(1)
O+O ₃ → O ₂ +O ₂	8.0×10^{-12}	-2060	(1)
O+O+M → O ₂ +M	9.4×10^{-34}	484	(1)
O+OH → O ₂ +H	2.2×10^{-11}	120	(1)
O ₃ +OH → HO ₂ +O ₂	1.6×10^{-12}	-940	(1)
H+O ₃ → OH+O ₂	1.4×10^{-10}	-470	(1)
H+O ₂ +M → HO ₂ +M	5.7×10^{-32}	-1.6	(1)
H ₂ O+O ¹ D → OH +OH	2.2×10^{-10}	0.0	(1)
H+HO ₂ → H ₂ +O ₂	1.6×10^{-12}	0.0	(1)
OH+HO ₂ → H ₂ O+O ₂	4.8×10^{-11}	250	(1)
O+HO ₂ → O ₂ +OH	3.0×10^{-11}	200	(1)
O ₂ +hν → O+O			(2)
O ₂ +hν → O+O(¹ D)			(2)
O ₃ +hν → O ² +O(¹ D)			(2)
O ₃ +hν → O ² +O(³ P)			(2)
H ₂ O+hν → H+OH			(3)
H ₂ O+hν → H ₂ +O(¹ D)			(3)

Sources: 1, JPL [2000]; 2, Nicolet [1984b]; 3, Nicolet [1984a].

^aRates are of the form $k = Ce^{A/T}$, where T is the temperature in K, and k is in units of molecule cm s.

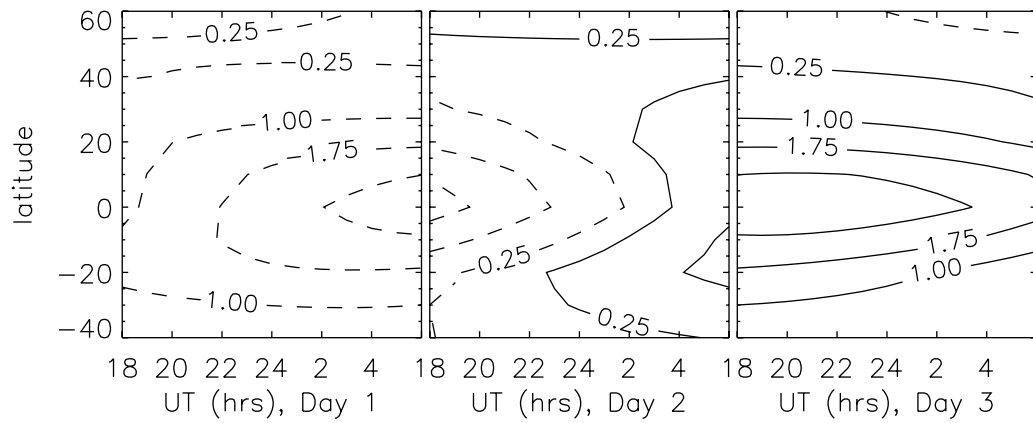


Figure 1. Latitude-time structure of the Kelvin wave vertical wind field at 96 km and 0° longitude. Contours are in units of cm s^{-1} .

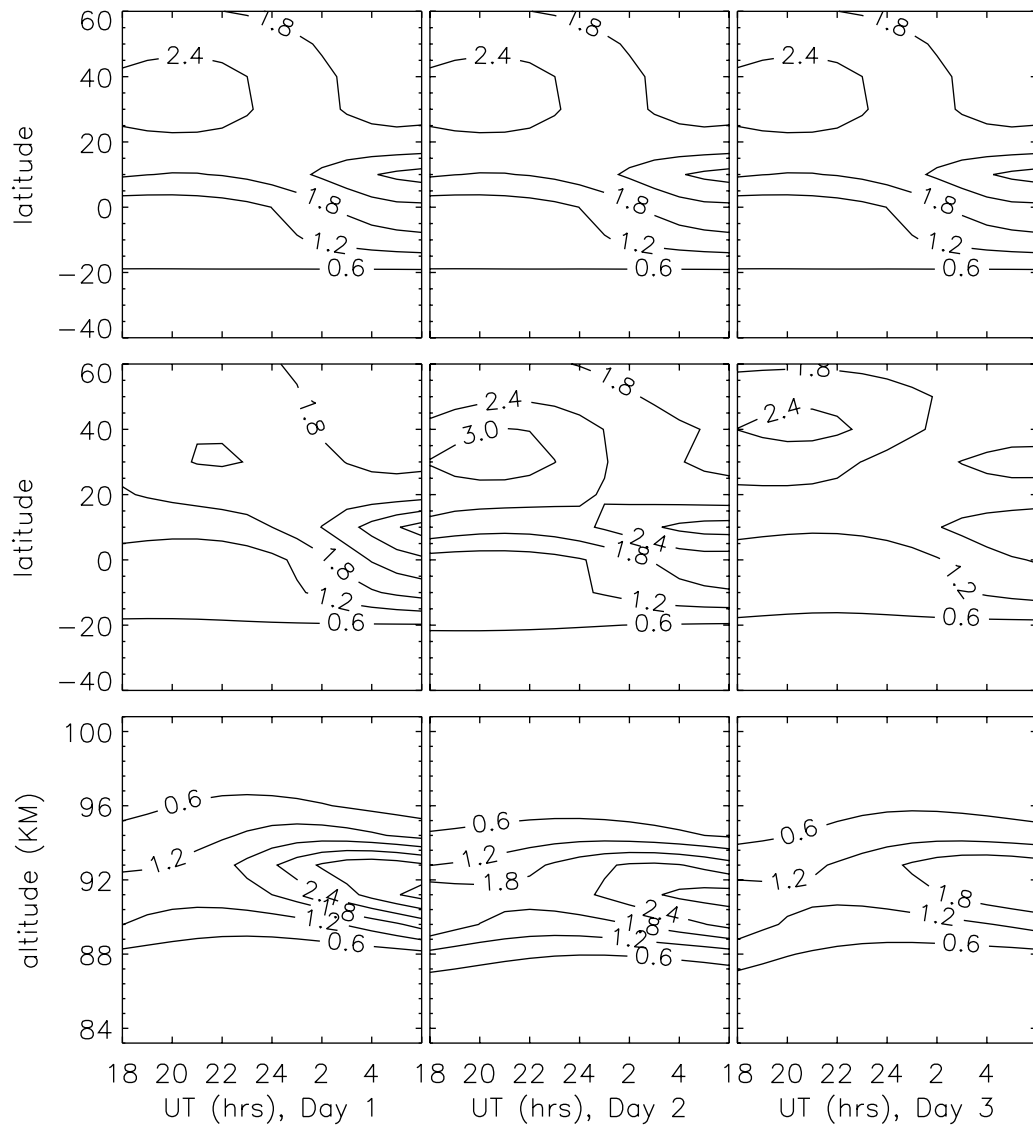


Figure 2. Latitude-time structure of the greenline emission at 96 km for three consecutive days, with diurnal and semidiurnal tides only (top), and with Kelvin wave effects (middle). The bottom panels illustrate the height-time structure of the greenline emission at 20° latitude including Kelvin and tidal effects. All contours are at 0° longitude. Contours are in units of $10^2 \text{ photons cm}^{-3} \text{ s}^{-1}$.

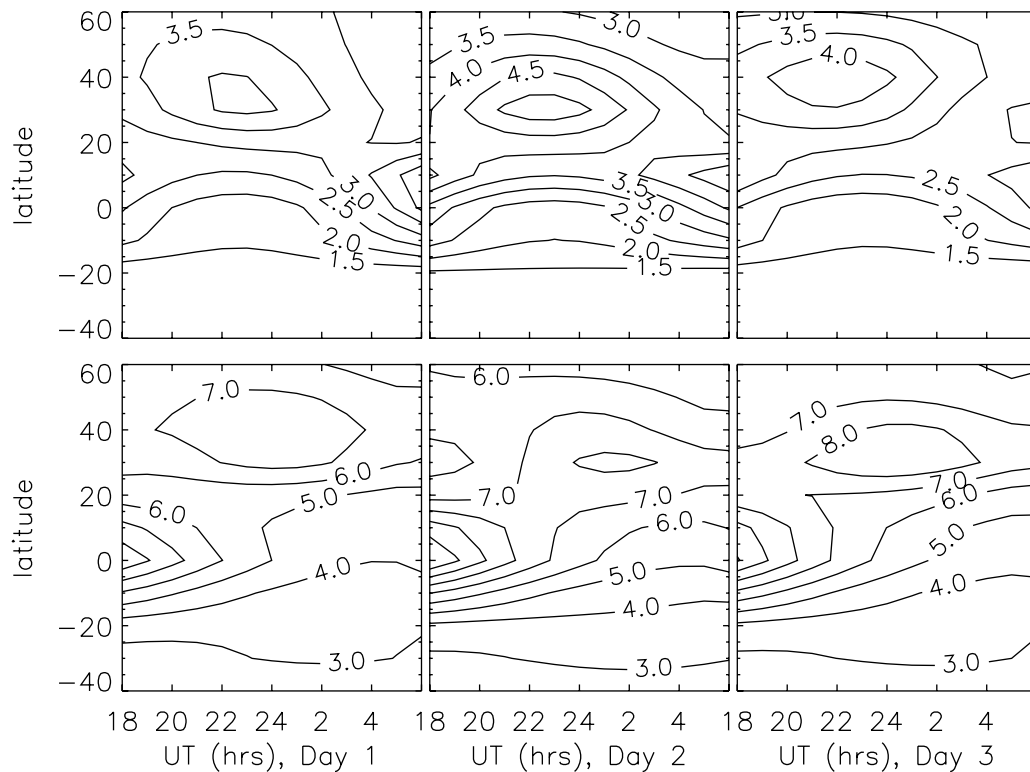


Figure 3. Latitude-time structures of the $O_2(0,1)$ (top panels) and $OH(6,2)$ emissions (bottom panels) for three consecutive nights at the respective peak heights of 98 and 88 km at 0° longitude. Contours are in units of 10^2 photons $cm^{-3} s^{-1}$.

velocity components due to eddy and molecular diffusion and the Kelvin wave. Meridional winds are small for the Kelvin wave. Simple scale analysis of the above equation shows that the omitted zonal transport term is of the same order as the vertical advection term, so that the results presented here only represent a first-order approximation.

[5] Chemistry in the model utilizes the family technique, in which constituents are grouped into chemically coupled families. Concentrations for chemically active species are derived from chemical partitioning at equilibrium. Chemical reactions that are included are listed in Table 1. Photochemical reaction rates are taken from Nicolet [1984a, b] and chemical rates are from JPL [2000]. Calculation of the greenline and O_2 atmospheric band emission rates assume a Barth transfer mechanism for chemical excitation [McDade *et al.*, 1986], giving the greenline a cubic dependence on $[O]$, and the O_2 atmospheric band a quadratic one. We simulate the $O_2(0,1)$ band to facilitate comparison with the data. The OH emission observed over Brazil originates from $OH(6,2)$. A proper treatment [Makhlouf *et al.*, 1995] would require simultaneous solution of a large number of excited OH species within the chemical scheme. In the present work, we use a formula developed by McDade and Llewellyn [1987] to calculate the $OH(8,3)$ rate, and then multiply this result by the steady-state ratio of the $OH(6,2)$ and $OH(8,3)$ emissions [Takahashi and Batista, 1981], making the assumption that the period of the 3.5-day oscillation is long enough to neglect any deviation from this steady-state ratio.

[6] Transport includes eddy and molecular diffusion, vertical motions due to diurnal and semi-diurnal tides, and the Kelvin Wave. Kelvin wave temperature and density perturbations are also included in the reaction rates, but as was found for the diurnal tide [Angelats *i Coll and Forbes*, 1998], vertical winds are the dominant contributor to airglow oscillations. Figure 1 illustrates the vertical wind field utilized in the model at a height of 96 km.

Vertical velocities for the equatorially-trapped Kelvin wave are maximum at the equator.

3. Model Results

[7] The top two rows of panels in Figure 2 show the latitude vs. time distributions of the greenline emission at 96 km with and without Kelvin wave effects for three consecutive nights. The structural features in the top panel, in particular the decrease in emission rate near midnight in the equatorial region, is due primarily to the effects of the migrating diurnal tide. The modulation of these features due to the Kelvin wave with 3-day period are clearly seen in the middle panel. Modifications of the patterns on the order of $\pm 25\%$ are discernable. The bottom panel of Figure 2 similarly shows the modulating effect of the Kelvin wave on the height-time structure of the greenline emission. The latitude-time structures of the O_2 atmospheric and OH Meinel emission rates are shown in Figure 3, again clearly exhibiting effects of the Kelvin wave.

[8] It is interesting to note that although the Kelvin wave vertical velocities are roughly an order of magnitude less than those of the diurnal tide examined in Angelats *i Coll and Forbes* [1998], the airglow variations in this study are comparable in magnitude, owing to the comparatively long period of the Kelvin wave.

4. Comparison with Airglow Observations

[9] The airglow observations were made using a multi-channel, tilting-filter zenith airglow photometer. Atomic oxygen 5577Å and 6300Å, NaD 5893Å, $O_2(0,1)$ atmospheric band and $OH(6,2)$ Meinel band emissions, as well as OH temperature measurements were taken for 140 nights spanning January to December 1998. An

overview of these observations, and details of experimental techniques and data processing, are described in *Takahashi et al.* [2001]. Herein, we concentrate on the data for June and July, 1998, which exhibited a 3.5-day variation in the greenline, OH and O₂ emissions.

[10] The 3.5-day variations in height-integrated intensity, expressed as a peak-to-peak percent variation about the mean value, are 40%, 28% and 22% for the simulated 5577Å, O₂(0,1), and OH(6,2) emissions, respectively. These values are insensitive to the phase of the Kelvin wave with respect to local time. This compares favorably with the respective observational values of 40%, 23%, and 26%. Furthermore, the magnitude of the temperature perturbation seen in the data (6°K at 88 km) is nearly identical to that obtained by the model of *Forbes* [2000]. This fact, when viewed in conjunction with the agreement in variations of airglow intensity, supports the consistency of the airglow observations with a Kelvin wave interpretation.

[11] A comparison of the data for 1998 and 1999 featured in *Takahashi et al.* [2001] indicates that there is yearly variability in the magnitude of the 3 day oscillation for the O₂ and OH emissions. It is speculated that this could be due to interaction between the Kelvin wave and tides, and interannual variability in tropical convective processes. Further modeling efforts would benefit by addressing these additional facets.

5. Conclusions

[12] A one-dimensional dynamical-chemical simulation demonstrates that the quasi-3-day Kelvin wave can induce ~22–40% variations in greenline, OH Meinel, and O₂ atmospheric band height-integrated emission rates in the MLT region. The effects are mainly induced by vertical velocities associated with the Kelvin wave dynamics. Ground-based zenith airglow photometer measurements near the equator reveal similar-amplitude oscillations in the same emissions. Other satellite and radar measurements indicate that the quasi-3-day wave in the equatorial region is an eastward-propagating Kelvin wave with zonal wavenumber $s = 1$. The airglow measurements are therefore interpreted as a manifestation of this “ultra-fast” Kelvin wave, and to our knowledge is the first reported connection between tropospheric convective processes and emissions in the MLT region. Future works should examine the effects of zonal transport on Kelvin wave emissions, which have been neglected in the present one-dimensional treatment.

[13] **Acknowledgments.** This work was supported under Grant NAG5-4467 from NASA Headquarters to the University of Colorado.

References

- Angelats i Coll, M., and J. M. Forbes, Dynamical influences on atomic oxygen and 5577 Å emission rates in the lower thermosphere, *Geophys. Res. Lett.*, 25, 461–464, 1998.
- Forbes, J. M., Wave coupling between the upper and lower atmosphere: case study of an ultra-fast Kelvin wave, *J. Atmos. Terr. Phys.*, 62, 1603–1621, 2000.
- Hedin, A. E., Extension of the MSIS thermosphere model into the middle and lower atmosphere, *J. Geophys. Res.*, 96, 1159–1172, 1991.
- Jet Propulsion Laboratory, Chemical kinetics and photochemical data for stratospheric modeling, *JPL Publications*, 00–3, 2000.
- Longuet-Higgins, M. S., The eigenfunctions of Laplace’s tidal equation over a sphere, *Phil. Trans. Roy. Soc. Lond.*, A262, 511–607, 1968.
- Makhlouf, U. B., R. H. Picard, and J. R. Winick, Photochemical-dynamical modeling of the measured response of airglow to gravity waves. 1: Basic model for OH airglow, *J. Geophys. Res.*, 100, 11,289–11,311, 1995.
- McDade, I. C., D. P. Murtaugh, R. G. H. Greer, P. G. H. Dickinson, G. Witt, J. Stegman, E. J. Llewellyn, L. Tomas, and D. B. Jenkins, Eton2: Quenching parameters for the proposed precursors of O₂ and O in the terrestrial nightglow, *Planet. Space Sci.*, 34, 789–795, 1986.
- McDade, I. C., and E. J. Llewellyn, Kinetic parameters related to sources and sinks of vibrationally excited OH in the nightglow, *J. Geophys. Res.*, 92, 7643–7659, 1987.
- Nicolet, M., On the photodissociation of water vapour in the mesosphere, *Planet. Space Sci.*, 32, 871–879, 1984a.
- Nicolet, M., Photodissociation of molecular oxygen in the terrestrial atmosphere: simplified numerical relations for the spectral range of the Schumann-Runge bands, *J. Geophys. Res.*, 89, 2573–2581, 1984b.
- Salby, M. L., D. L. Hartman, P. L. Bailey, and J. C. Gille, Evidence for equatorial Kelvin waves in Nimbus-7 LIMS, *J. Atmos. Sci.*, 41, 220–235, 1984.
- Takahashi, H., and P. P. Batista, Simultaneous measurements of OH(9,4), (8,3), (7,2), (6,2), and (5,1) bands in the airglow, *J. Geophys. Res.*, 86, 5632–5642, 1981.
- Takahashi, H., R. A. Buriti, D. Gobbi, and P. P. Batista, Equatorial planetary waves observed by the mesospheric airglow emissions, *J. Atmos. Solar-Terr. Phys.*, in press, 2001.
- D. Gobbi, Instituto Nacional de Pesquisas Espaciais (INPE) São José dos Campos SP, Brasil.
- H. Takahashi, Instituto Nacional de Pesquisas Espaciais (INPE) São José dos Campos, SP, Brasil. (hisao@laser.inpe.br)
- M. Angelats i Coll, Department of Aerospace Engineering Sciences University of Colorado Campus Box 429 Boulder, CO 80309-0429. (angel@odo.colorado.edu)
- J. M. Forbes, Department of Aerospace Engineering Sciences University of Colorado Campus Box 429 Boulder, CO 80309-0429. (forbes@zke.colorado.edu)
- G. S. Lichstein, Department of Aerospace Engineering Sciences University of Colorado Campus Box 429 Boulder, CO 80309-0429. (lichstei@odo.colorado.edu)
- R. A. Buriti, Universidade Federal da Paraíba Campina Grande PB, Brasil. (rburitiit@df.ufpb.br)